Aftershocks' Effect on Structural Design Actions in Italy

Aftershocks' Effect on Structural Design Actions in Italy

Iunio Iervolino,[1] Eugenio Chioccarelli,[2] and Massimiliano Giorgio.[3]

[1]*Dipartimento di Strutture per l'Ingegneria e l'Architettura, Università degli Studi di Napoli Federico II, via Claudio 21, 80125, Naples, Italy.* iunio.iervolino@unina.it
[2]*Università Telematica Pegaso, piazza Trieste e Trento 48, 80132 Naples, Italy*.
eugenio.chioccarelli@unipegaso.it
[3]*Dipartimento di Ingegneria Industriale e dell'Informazione, Università degli Studi della Campania Luigi Vanvitelli, via Roma 29, 80131, Aversa (CE), Italy.* massimiliano.giorgio@unicampania.it

Abstract

Although earthquakes generally form clusters both in space and time, only mainshocks, usually the largest magnitude events within a cluster, are considered by probabilistic seismic hazard analysis (PSHA; Cornell, 1968). On the other hand, aftershock probabilistic seismic hazard analysis (APSHA), based on the modified Omori law, allows the quantification of the aftershock threat (Yeo and Cornell, 2009). Classical PSHA often describes event occurrence via a homogeneous Poisson process, whereas APSHA describes occurrence of aftershocks' via cluster-specific nonhomogeneous Poisson processes, the rate of which is a function of the mainshock magnitude. It is easy to recognize that clusters, each of which is made of the mainshock and the following aftershocks, occur at the same rate of mainshocks. This recently allowed the generalization of the hazard integral to account for aftershocks in PSHA (i.e., Iervolino et al., 2014), which resulted in the formulation of the so-called sequence-based probabilistic seismic hazard analysis (SPSHA). In the present study, SPSHA is applied to Italy countrywide, using the same source model (Stucchi et al., 2011) lying at the basis of the official PSHA used for structural design, to quantitatively assess the increase in seismic design actions for structures when accounting for the aftershocks.

Introduction

The state-of-the-art in structural engineering codes is such that design seismic accelerations are derived from probabilistic seismic hazard analysis (PSHA; Cornell, 1968, McGuire, 2004). The latter provides, for a site of interest, the ground motion intensity measure (*IM*) value that corresponds to a given rate of

exceedance. The *IM* is typically an ordinate of a pseudo-acceleration response spectrum, and structures must be designed against values corresponding to rates that are functions of the desired seismic performance.

Even if seismic events generally occur in time-space clusters, classical PSHA describes the occurrence of earthquakes via a homogeneous Poisson process or HPP. (This model is used to determine seismic design actions in Italy, that is the case investigated herein; however, other occurrence processes can be used for PHSA, see for example Beauval et al., 2006). From the HPP assumption of earthquake occurrence, it follows that the events causing the exceedance of an *IM*-value at a site of interest occur according to a HPP (Cornell, 1968). To be compatible with this modeling hypothesis, only mainshocks, typically the largest magnitude earthquakes within each cluster, are considered via procedures generally known as catalog declustering (e.g., Gardner and Knopoff, 1974).

For short-term risk management purposes during seismic sequences, aftershock probabilistic seismic hazard analysis (APSHA) has been developed (Yeo and Cornell, 2009). APSHA models the occurrence of aftershock via cluster-specific nonhomogeneous Poisson processes (NHPP), the rate of which is a function of the magnitude of the mainshock that has triggered the sequence, via the modified Omori law (Utsu, 1961). Because earthquake sequences, made of mainshocks and following aftershocks, occur at the same rate of the mainshocks, it is possible to combine HPP-based PSHA and APSHA to include the effect of aftershocks in probabilistic seismic hazard analysis, still working with a declustered catalog. The mathematics of this stochastic model, named sequence-based probabilistic seismic hazard analysis (SPSHA), was presented in Iervolino et al. (2014).

For any given *IM*-value, SPSHA provides the rate of mainshock-aftershock clusters that cause its exceedance at the site, and its main advantages are: (i) it is probabilistically rigorous in the framework of PSHA and APSHA, (ii) it allows the retention of the HPP hypothesis for their occurrence, and (iii) it avoids the issues of non-declustered catalogs such as completeness (see also Marzocchi and Taroni, 2014). It should also be noted that SPSHA, although stimulated by the work of Boyd (2012), is different mainly because it does not consider foreshocks, makes recourse to APSHA to describe aftershocks, and provides an analytical framework extending the classical PSHA integral.

To quantify the effect of aftershocks on design accelerations, SPSHA is applied herein to Italy to develop maps of two spectral (pseudo) accelerations corresponding to four return periods, those that are most common for design of structures according to the Italian seismic code (Stucchi et al., 2011). To this aim, the same source model (i.e., Meletti et al., 2008) of the current official seismic hazard of Italy is considered. The obtained SPSHA maps are compared with those based on the same source model, yet from classical PSHA, to help in quantitatively assessing the effects of aftershocks for structural design, a relevant issue from the earthquake engineering perspective.

The remainder of the paper is structured such that the essentials of SPSHA are recalled first. Then, disaggregation of SPSHA, not originally provided in Iervolino et al. (2014) is formulated. It allows the assessment of how much the exceedance of a ground motion *IM*-value is contributed by aftershocks with respect to mainshocks, and is helpful for the scopes of this study. Subsequently, after introducing the considered source model for Italy, SPSHA results, in terms of countrywide maps of spectral accelerations for given return periods of exceedance, are presented along with the PSHA counterpart. Moreover, two sites, exposed to comparatively low and high hazard according to PSHA, are also considered for more detailed discussions. The modeling consistency between PSHA and SPSHA allows, finally, the direct comparison of the obtained results and the discussion of the engineering significance of accounting for aftershocks in seismic hazard assessment in Italy.

Sequence-based probabilistic seismic hazard analysis

The main result of PSHA for a site of interest is the average number of earthquakes in one year (i.e., the rate) causing exceedance of a given *IM* threshold, say *im*. The rate of exceedance of *im*, herein indicated as $\lambda_{im,E}$, is typically obtained via Equation (1), which is written, for simplicity, for the case of a single seismic source zone.

$$\lambda_{im,E} = \nu_E \cdot \int_{r_{E,\min}}^{r_{E,\max}} \int_{m_{E,\min}}^{m_{E,\max}} P\left[IM_E > im \mid x, y\right] \cdot f_{M_E,R_E}\left(x, y\right) \cdot dx \cdot dy \quad (1)$$

In the equation, ν_E is the rate, from a declustered catalog (e.g., Reiter, 1990), of earthquakes above a minimum magnitude of interest $\left(m_{E,\min}\right)$ and below the maximum magnitude $\left(m_{E,\max}\right)$ of the considered seismic source. The term $P\left[IM_E > im \mid x, y\right]$, provided by a ground motion prediction equation (GMPE), represents the probability that the intensity threshold is exceeded given an earthquake of magnitude $M_E = x$, from which the site is separated by a distance $R_E = y$, where $R_E \in \left(r_{E,\min}, r_{E,\max}\right)$. The term f_{M_E,R_E} is the joint probability density function (PDF) of mainshock magnitude and distance random variables (RVs). If these two RVs may be considered stochastically independent, f_{M_E} can be, for example, described by a truncated exponential distribution, derived by the Gutenberg-Richter (GR) relationship (Gutenberg and Richter, 1944), and f_{R_E} is obtained on the basis of the source-site geometrical configuration. The integral limits are the magnitudes bounding the magnitude PDF and the distances defining the domain of possible R_E values.

Because ν_E is from a declustered catalog, and f_{M_E,R_E} refers to mainshocks, then the subscript (E) was added to distinguish the obtained rate, $\lambda_{im,E}$, from the one by SPSHA, to follow. Finally, in the case of multiple seismic source, say *s* in number, Equation (1) is computed one source at a time and the results summed up: $\lambda_{im,E} = \sum_{i=1}^{s} \lambda_{im,E,i}$.

SPSHA aims to evaluate the average number of seismic sequences (mainshocks and following aftershocks) that in one year cause at least one exceedance of *im* at the site. This rate, called λ_{im}, is still that of a HPP. It was demonstrated in Iervolino et al. (2014) that, under the hypotheses for aftershock hazard of Yeo and Cornell (2009), λ_{im} can be computed via Equation (2); i.e., a generalization of Equation (1).

$$\lambda_{im} = \nu_E \cdot \left\{ 1 - \iint_{M_E,R_E} P\left[IM_E \le im \mid x, y\right] \cdot e^{-E\left[N_{A|x}(0,\Delta T_A)\right] \cdot \iint_{M_A,R_A} P\left[IM_A > im \mid w,z\right] \cdot f_{M_A,R_A|M_E,R_E}(w,z) \cdot dw \cdot dz} \cdot f_{M_E,R_E}(x,y) \cdot dx \cdot dy \right\} \qquad (2)$$

The terms: ν_E, $P\left[IM_E \le im \mid x, y\right] = 1 - P\left[IM_E > im \mid x, y\right]$, and $f_{M_E,R_E}(x,y)$ are the same as defined in Equation (1). Also $M_E \in \left(m_{E,\min}, m_{E,\max}\right)$ and $R_E \in \left(r_{E,\min}, r_{E,\max}\right)$; i.e., the integral limits are also the same.

The exponential term within the integral refers to aftershocks and is worth of a description. It is the probability that none of the aftershocks, following the mainshock of features $\{M_E = x, R_E = y\}$, cause exceedance of *im*. This probability depends on $P[IM_A > im \mid w, z]$ that is the probability that *im* is exceeded given an aftershock of magnitude $M_A = w$ and source-to-site distance $R_A = z$. The term $f_{M_A,R_A|M_E,R_E}$ is the distribution of magnitude and distance of aftershocks, which are conditional on the features $\{M_E, R_E\}$ of the mainshock. This distribution can be written as $f_{M_A,R_A|M_E,R_E} = f_{M_A|M_E} \cdot f_{R_A|M_E,R_E}$, where $f_{M_A|M_E}$ is the PDF of aftershock magnitude (i.e., GR-type), and $f_{R_A|M_E,R_E}$ is the distribution of the distance of the site to the aftershocks. The aftershock magnitude is bounded by a minimum magnitude, $m_{\min}$, and the mainshock magnitude; i.e., $M_A \in (m_{\min}, x)$. (Note that $m_{\min}$ may coincide with the minimum mainshock magnitude; i.e., $m_{\min} \equiv m_{E,\min}$.) Given the location of the site, the aftershock distance, $R_A \in (r_{A,\min}, r_{A,\max})$, depends on the magnitude and location of the mainshock (see Iervolino et al., 2014, for details). $E[N_{A|x}(0, \Delta T_A)]$ is the expected number of aftershocks, to the mainshock of magnitude $M_E = x$, in the ΔT_A time interval, which is the considered length of the aftershock sequence (assuming that the mainshock occurred at $t = 0$). This number, consistent with APSHA, can be computed as in Equation (3), where $\{a, b, c, p\}$ are the parameters of the modified Omori law (Yeo and Cornell, 2009).

$$E[N_{A|x}(0, \Delta T_A)] = \frac{10^{a+b\cdot(x-m_{\min})} - 10^{a}}{p-1} \cdot \left[c^{1-p} - (\Delta T_A + c)^{1-p}\right] \tag{3}$$

In fact, Equation (2) represents a hazard integral for aftershocks (exponential term), conditional to $M_E = x$ and $R_E = y$, nested in a classical PSHA integral. It is easy to recognize that it must be $\lambda_{im} \geq \lambda_{im,E}$; i.e., accounting for aftershocks necessarily increases the hazard. Moreover, Equation (2) precisely degenerates in Equation (1) in case aftershocks are neglected; i.e., $E[N_{A|x}(0, \Delta T_A)] = 0, \forall x \in (m_{E,\min}, m_{E,\max})$. Thus, the latter equation generalizes the former.

Finally, it should be noted that, for design, earthquake engineering is interested in the probability that at least one exceedance of a ground motion intensity measure is observed during the design-life of the structure, ΔT . In SPSHA, because the computed rate is still that of an HPP, such a probability can be computed via $1-e^{-\lambda_{im}\cdot\Delta t}$, exactly as in the PSHA case. Thus, design seismic actions can be updated accounting for the aftershock effect within the classical probabilistic framework.

Aftershock disaggregation

A side result of SPSHA formulation, is the probability that exceedance of *im* is caused by an aftershock rather than by a mainshock. This probability, which quantifies the contribution of aftershocks to hazard, can be regarded as a disaggregation in much the same way classical hazard disaggregation (e.g., Iervolino et al., 2011) provides the probability that exceedance of design accelerations is caused by specific magnitude-distance pairs, or other random variables possibly involved in the hazard assessment.

SPSHA disaggregation is defined in Equation (4) as $P\left[IM_{\cup A}>im\cap IM_E\le im\middle|IM_{\cup A}>im\cup IM_E>im\right]$. The symbol IM_E represents the mainshock *IM*, while $IM_{\cup A}$ is the maximum *IM* of the following aftershock sequence. Then, the sought probability is the probability that, given that exceedance of *im* has been observed during the mainshock-aftershock sequence due to the mainshock or at least one of the aftershocks, that is $\left(IM_E>im\cup IM_{\cup A}>im\right)$, it was in fact an aftershock to cause it, while the mainshock was below the threshold: i.e., $\left(IM_{\cup A}>im\cap IM_E\le im\right)$.

$$P\left[IM_E\le im\cap IM_{\cup A}>im\middle|IM_E>im\cup IM_{\cup A}>im\right]=$$
$$\frac{\nu_E}{\lambda_{im}}\cdot\iint_{M_E,R_E}P\left[IM_E\le im\,|\,x,y\right]\cdot\left(1-e^{-E\left[N_{A|x}\left(0,\Delta T_A\right)\right]\cdot\iint_{M_A,R_A}P\left[IM_A>im|w,z\right]\cdot f_{M_A,R_A|M_E,R_E}\left(w,z\right)\cdot dw\cdot dz}\right)\cdot f_{M_E,R_E}\left(x,y\right)\cdot dx\cdot dy \quad (4)$$

The equation, the derivation of which is given in the appendix, uses terms already introduced to define SPSHA. It will be useful for the scope of this work, as illustrated in the following countrywide application to Italy.

SPSHA for Italy

Mainshock model (classical hazard)

The source model considered herein for Italy is the one by Meletti et al. (2008), which features thirty-six seismic source zones (Figure 1) and lies at the core of the Italian hazard study described in Stucchi et al. (2011). The latter, in turn, provides uniform hazard spectra (UHS) to define engineering structural seismic actions according to the enforced code.

The seismic hazard study of Stucchi et al. (2011) features a fairly-complex logic tree. Herein, the branch named 921 is considered; it is the single branch producing the hazard results claimed to be the closest to those of the full logic tree (this is for simplicity only, as modeling uncertainty can be considered in SPSHA in analogy to what done in PSHA). Branch 921 considers the mentioned zones and the GMPE by Ambraseys et al. (1996) to compute $P\left[IM_E > im \mid x, y\right]$ on rock soil conditions.

Herein, the GMPE is applied within its definition ranges of magnitude and distance: these are magnitudes between 4.0 and 7.5 and the closest horizontal distance to the surface projection of the fault plane up to 200 km. The effects of earthquakes with magnitude and distance outside these intervals are neglected. Assuming a uniform epicenter distribution in each seismogenic zone, epicentral distance is converted into the metric required by the GMPE according to Montaldo et al. (2005). The style-of-faulting correction factors proposed by Bommer at al. (2003) are also applied to the GMPE, consistent with the rupture mechanism associated to each seismic source zone by Meletti et al. (2008).

As it regards the mainshock rates of the zones, in branch 921 of Stucchi et al. (2011) they are not provided as GR relationships, but for surface-wave magnitude bins. These, provided by Carlo Meletti (see Data and Resources), are given in Table 1. The central magnitude of the lowest bin is generally 4.3 (apart from the zone 936 which is the Etna's volcanic area and has a central magnitude of the lower bin equal to 3.7), while the maximum depends on the zone of interest (as it can be inferred from the largest magnitude bin with rate larger than zero in Table 1).

This model is used either to compute PSHA for the country (to provide a point of comparison), as well as to compute SPSHA, which considers the same mainshock rates and zones.

Aftershock model

The parameters used in the modified Omori law, Equation (3) are from Lolli and Gasperini (2003) for generic Italian aftershock sequences: $a = -1.66$, $b = 0.96$, $c = 0.03$ (in days), $p = 0.93$. The minimum magnitude of generated aftershocks $(m_{\min})$ corresponds to the minimum mainshock magnitude of the seismic source zones: that is, 4.15 for all the seismogenic zones, except zone 936 for which it is 4.0. Indeed, zone 936 is able to generate earthquakes with magnitude lower than 4.0; however, the GMPE is applied within its definition range, which constrains the aftershocks' minimum magnitude to 4.0.

It is assumed that aftershocks are located, with uniform probability, in a circular area centered on the mainshock location. The size of this area, S_A, depends on the magnitude of the mainshock $(M_E = x)$ via Equation (5), in squared kilometers (Utsu, 1970).

$$S_A = 10^{x-4.1} \tag{5}$$

Working hypotheses

Some working hypotheses that were taken mostly for simplicity, are believed not to affect the general conclusions; nevertheless, they could be possibly refined in more detailed studies.

The aftershock area is considered circular for simplicity, although an elliptical shape, for example along the Apennines mountain chain (in central Italy) that is the typical strike orientation in the region, would better reflect knowledge of seismicity. Within the aftershock area, locations are uniformly distributed, while their probability is zero outside. On the other hand, an aftershock probability gradually decreasing as the distance from the mainshock increases is often preferred (it was verified in Iervolino et al., 2014, that this hypothesis negligibly affects the results). Moreover, the limits of the aftershock area can exceed the boundaries of the seismic source zone.

Equation (5) was originally calibrated for $5.5 < M_E < 7.5$; in the applications shown in this paper, it is extended to the minimum magnitudes considered. The Ambraseys et al. (1996) GMPE is used for both $P[IM_A > im \mid w, z]$ and $P[IM_E \le im \mid x, y]$ terms of Equation (2); i.e., for both mainshock and aftershocks, also keeping the same style of faulting recommended for the zone in question by Meletti et al. (2008).

Finally, following Yeo and Cornell (2009), the duration of the aftershock sequence (ΔT_A) was considered arbitrarily equal to ninety days since the occurrence of the mainshock, although, in principle, this duration could be mainshock-magnitude-dependent. In any case, it has been verified that assuming $\Delta T_A = 365$ days leads to negligible differences in results compare to $\Delta T_A = 90$ days.

Analysis and results

In the following sections, SPSHA results for Italy are presented along with their PSHA counterpart (all calculations are carried out via a recent version of the software described in Iervolino et al., 2016). First, hazard maps are reported for several return periods and two spectral ordinates. Then, considering two specific sites, hazard curves, uniform hazard spectra and aftershock disaggregation are provided and discussed.

Hazard maps

To compute hazard maps, a uniformly-spaced grid of more than four-thousand points covering the inland Italian territory is considered. Peak ground acceleration (PGA) and spectral accelerations at 1 second natural vibration period, $Sa(1\text{s})$, on rock, are considered as the *IMs*. The hazard maps refer to four return periods (T_r): 50yr, 475yr, 975yr and 2475yr. Results are reported in Figure 2 and Figure 3, for PGA and $Sa(1\text{s})$ respectively. In each figure, the upper line of panels, that is maps from (a) to (d), result from PSHA. The lower line, maps from (e) to (h), are the corresponding results from SPSHA. To compare PSHA and SPSHA for the same return period in both figures, one should consider panels: (a) and (e) for $T_r = 50\text{yr}$, (b) and (f) for $T_r = 475\text{yr}$, (c) and (g) for $T_r = 975\text{yr}$, (d) and (h) for $T_r = 2475\text{yr}$. It can be preliminary observed that, in general, the effect of aftershocks tends to be more relevant in areas exposed to comparatively high hazard according to classical PSHA; i.e., areas with larger acceleration values in the top panels of Figure 2 and Figure 3.

To more quantitatively assess the hazard increase due to aftershocks, Figure 4 shows absolute differences between SPSHA and PSHA in terms of *IM*s that, at the same site, correspond to the same return period (for example, panel (a) of Figure 4 is the map obtained subtracting the map in panel (a)

222 from that of panel (e) in Figure 2). Figure 5 reports the percentage increase; i.e., it is obtained by dividing
223 the maps in Figure 4 by the corresponding PSHA maps of Figure 2 and Figure 3. It can be observed
224 that: (i) absolute differences are generally larger for larger return periods; (ii) considering the same
225 return period, differences in terms of PGA are larger than those in terms of $Sa(1\text{s})$; (iii) considering the
226 same return period and the same intensity measure, largest differences are recorded at the sites enclosed
227 into the zone with highest maximum magnitude, that is zones 923, 927, 929 and 935; (iv) percentage
228 increases are not monotonic as a function of T_r; (v) also percentage increases in terms of PGA are
229 generally larger than those in terms of $Sa(1\text{s})$.

230 Table 2 summarizes average and maximum percentage differences (ave. perc. diff. and max.
231 perc. diff., respectively) over the country and maximum absolute differences (max. abs. diff.) from the
232 maps of Figure 4 and Figure 5. Average percentage increases for $Sa(1\text{s})$, as a function of the return
233 period, are between 10.4% and 7%, with the largest value occurring for $T_r = 50\text{yr}$. The range for PGA
234 is similar, that is around 10%, yet narrower. The maximum percentage increases are about 28% for PGA
235 at $T_r = 2475\text{yr}$ and 17% for $Sa(1\text{s})$ at $T_r = 475\text{yr}$. The former occurs just outside zone 935, while the
236 latter within it. It is interesting to note that, for $Sa(1\text{s})$, maximum increase does not correspond to the
237 largest return period. This issue is looked at deeper in the following sections in which two specific sites
238 are considered and site-specific hazard curve, uniform hazard spectra and aftershock disaggregation are
239 reported and discussed. Maximum absolute differences for PGA are equal to 0.012g, 0.058g, 0.084g
240 and 0.116g for return periods equal to 50yr, 475yr, 975yr and 2475yr, respectively. Maximum
241 differences in terms of $Sa(1\text{s})$ are equal to 0.007g, 0.035g, 0.051g and 0.075g for return periods equal
242 to 50yr, 475yr, 975yr and 2475yr, respectively. For PGA, the maximum differences for return periods
243 up to 975yr correspond to sites located within zone 929, while the maximum difference for $T_r = 2475\text{yr}$
244 occurs at a site enclosed into zone 935; for $Sa(1\text{s})$, maximum differences for $T_r = 50\text{yr}$ and $T_r = 475\text{yr}$
245 occur within zone 929, while they occur within the 935 zone for $T_r = 975\text{yr}$ and $T_r = 2475\text{yr}$ (see Figure
246 1).

Site-specific hazard analysis and aftershocks disaggregation

Two sites have been selected to analyse in more details the aftershocks effect on the hazard assessment. The sites are L'Aquila in central Italy (13.40°E, 42.35°N) and Milan in Northern Italy (9.18°E, 45.47°N): they are selected to be representative of the high (L'Aquila) and low (Milan) PSHA hazard according to classical PSHA (see Figure 2 and Figure 3).

Results for L'Aquila are given in Figure 6. More specifically, Figure 6a shows the site location and the fifteen seismogenic zones contributing to the hazard (i.e., within 200 km). The zone in which the site is enclosed is the 923, which is one of the three zones from Meletti et al. (2008) with largest maximum magnitude (the others are 929 and 935; see Table 1). In Figure 6b, the hazard curves for PGA (black lines) and $Sa(1\text{s})$ (grey lines) are reported (dashed is PSHA and solid is SPSHA). The range of *IM* in which the analyses are performed is such that the maximum return period is equal to ten thousand years. On the other hand, the maximum rate is 2.41, that is, the rate of mainshocks (then also clusters) occurring within 200km from the site; i.e., the rate of exceedance when *IM* tends to zero, see Equation (1) and Equation (2). Figure 6c reports the increase of *im* between SPSHA and PSHA as a function of the decreasing rate of exceedance (i.e., increasing return period). These differences are non-monotonic for both PGA and $Sa(1\text{s})$. Maximum increase for PGA is 17.9% and it occurs for a return period of 1350 years whereas the maximum increase for $Sa(1\text{s})$, equal to 12.6%, corresponds to a return period of about 530 years. The non-monotonic trend of hazard increase motivates the evidence that maximum increase for $Sa(1\text{s})$ at a national scale occurs at a 475yr return period (see Table 2). Uniform hazard spectra for the four return periods of 50yr, 475yr, 975yr and 2475yr are reported in Figure 6d. The spectra, indicated as PSHA_{T_r} and SPSHA_{T_r}, are computed considering the forty-seven natural vibration (spectral) periods, *T*, between zero and two seconds provided by the adopted GMPE. Increase between SPSHA and PSHA for the selected return periods is reported in Figure 6e as a function of the spectral period. When the return period is 50yr, hazard increase is about 10% for all the vibration periods. On the other hand, for return periods of 475yr, 975yr and 2475yr, hazard increase is between 15% and 20% for spectral periods lower than 0.7s, and are between 10% and 15% for spectral periods larger than

0.7s. Finally, aftershock disaggregation is reported in Figure 6f as a function of the increasing return period. As discussed above, SPSHA disaggregation according to Equation (4) provides the probability that, once exceedance of *im* is observed, it is caused by an aftershock rather than a mainshock; in this sense, it may help in assessing the contribution of aftershock to hazard. Also these curves show a non-monotonic trend. The probability that exceedance of the *IM* threshold of interest is caused by aftershocks initially rises with the rising return period. The maximum values of probability from aftershock disaggregation are equal to 0.34 for PGA and 0.19 for $Sa(1\text{s})$, and correspond to $T_r = 1900\text{yr}$ and $T_r = 2000\text{yr}$, respectively. For longer return periods, aftershock disaggregation decreases. The difference in disaggregation curves for PGA and for $Sa(1\text{s})$ is such that at the lower return periods the contribution of aftershocks is similar for the two spectral ordinates, while at the larger return periods is larger for PGA than Sa(1s). This may provide insights for the trends observed in Figure 6e.

Figure 7 shows the analogous results for Milan. The site is not enclosed in any seismogenic zone and its hazard is affected by the zones reported in Figure 7a. The rates of earthquake occurrence above minimum magnitude (i.e., the value hazard curves tend to when *IM* tends to zero) is 1.40 and the considered maximum return period is, similarly to the previous case, ten-thousand years. Hazard curves for PGA and $Sa(1\text{s})$ are reported in Figure 7b while increases are in Figure 7c. In the latter, maximum values equal to 8.5% and 9.0% for PGA and $Sa(1\text{s})$, respectively. The corresponding return periods are six and ten years. Figure 7d shows the UHS for the four return periods. Hazard increase (Figure 7e) due to SPSHA with respect to PSHA is, for this site, between about 4% and 10% for all the vibration periods and return periods here considered. However, the largest increases are observed for the lower return periods, which is explained by the trend observed in Figure 7c for PGA and $Sa(1\text{s})$. Hazard disaggregation is reported in Figure 7f: maximum probability value for PGA is 0.22 and it corresponds to a return period of 1200 years whereas maximum $Sa(1\text{s})$ is 0.16 for an *im* threshold with 60 years exceedance return period. It should be noted that the maximum values of the probability that an aftershock is causative for exceedance in Milan are significantly lower with respect to the case of L'Aquila, mainly because the former site is outside any seismic source zone, while the latter is within

one of the most seismically relevant, as per Table 1. To deepen how the trends, observed at this and the other site considered, depend on an interplay of source-site configuration, the interested reader is referred to Chioccarelli et al. (2018).

Conclusions

Sequence-based probabilistic seismic hazard analysis (SPSHA) includes the aftershock's effect in probabilistic seismic hazard assessment. The modified hazard integral relies on the modified Omori law and is probabilistically rigorous in the framework of the considered models. The SPSHA stochastic model was introduced in 2014; herein it is applied at a national scale using Italy as a case-study. The hazard increase due to aftershocks is evaluated considering the same source model lying at the basis of the official seismic hazard of Italy used for structural design. Comparison was carried out in terms of maps of two spectral ordinates with four return periods of exceedance between 50yr and 2475yr on rock site conditions, as well as full hazard curves and SPSHA disaggregation for two sites differently exposed to seismic hazard according to classical PSHA. Beyond the obvious fact that accounting for the aftershocks' effect increases the hazard in Italy, the analysis allowed pointing out the following issues:

- increase of im for a given return period can be as high as about 30%; in absolute terms, up to 0.12g for PGA when the return period of the exceedance is 2475 years (the site for which the percentage increase is maximum is not the one for which the absolute increase is the largest);
- as expected, increase due to aftershocks tends to be more significant within or around areas exposed to comparatively higher hazard according to classical PSHA; however, increases are not analogous for different *IM*s; e.g., PGA and $Sa(1\text{s})$; as expected by the fact that magnitudes and source-to-site distances contribute differently to hazard of different spectral ordinates;
- disaggregation of sequence-based probabilistic hazard, at least in the considered examples, shows that the contribution of hazard is not monotonic with the increasing return period of exceedance (the specific trend at each site depends on the source-site configuration).

It may be concluded that, notwithstanding the working hypothesis behind this application, which could be refined in more detailed studies, introducing Omori-type aftershock sequences can have a non-negligible effect on design actions in Italy.

Data and resources

All data and resources used in this study are from the listed references, except magnitude rates, which were kindly provided by Carlo Meletti (Istituto Nazionale di Geofisica e Vulcanologia, Italy).

Acknowledgements

This work was developed within the *Rete dei Laboratori Universitari di Ingegneria Sismica* (ReLUIS) 2014-2018 framework programme. Authors thank Ms. Racquel K. Hagen (Stanford University, CA) for having proofread the manuscript.

References

Ambraseys, N. N., K. A. Simpson, and J. J. Bommer (1996). Prediction of horizontal response spectra in Europe, *Earthq. Eng. Struct. D.* **25**, 371-400.

Beauval, C., S. Hainzl, and F. Scherbaum (2006). Probabilistic seismic hazard estimation in low-seismicity regions considering non-Poissonian seismic occurrence, *Geophys. J. Int.* **164**, 543-550

Bommer, J. J., J. Douglas, and F. O. Strasser (2003). Style-of-faulting in ground-motion prediction equations, *Bull. Earthq. Eng.* **1**, 171–203.

Boyd, O. S. (2012). Including foreshocks and aftershocks in time-independent probabilistic seismic-hazard analyses, *Bull. Seismol. Soc. Am.* **102**, 909-917.

Chioccarelli, E., P. Cito, and I. Iervolino (2018). Disaggregation of sequence-based seismic hazard. Proc. of *16th Conference on Earthquake Engineering*, 16ECEE, Thessaloniki, Greece, 18-21 June.

Cornell, C. A. (1968). Engineering Seismic Risk Analysis, *B. Seismol. Soc. Am.* **58**, 1583-1606.

Gardner, J. K, L. Knopoff (1974). Is the sequence of earthquakes in southern California, with aftershocks removed, poissonian?, *Bull. Seismol. Soc. Am.* **60**(5), 1363–1367.

Gutenberg, B. and C. F. Richter (1944). Frequency of earthquakes in California, *B. Seismol. Soc. Am.* **34**, 185-188.

Iervolino, I., E. Chioccarelli, and P. Cito (2016). REASSESS V1.0: a computationally-efficient software for probabilistic seismic hazard analysis. Proc. of *VII European Congress on Computational Methods in Applied Sciences and Engineering, ECCOMAS*, Crete Island, Greece, 5–10 June.

Iervolino, I., M. Giorgio, and B. Polidoro (2014). Sequence-based probabilistic seismic hazard analysis. *Bull. Seismol. Soc. Am.* **104**, 1006-1012.

Iervolino, I., E. Chioccarelli, and V. Convertito (2011). Engineering design earthquakes from multimodal hazard disaggregation, *Soil Dyn. Earthq. Eng.* **31**(9), 1212–1231.

Lolli, B., and P. Gasperini (2003). Aftershocks hazard in Italy Part I: Estimation of time-magnitude distribution model parameters and computation of probabilities of occurrence, *J. Seismol.* **7**, 235–257.

Marzocchi, W., and M. Taroni (2014). Some thoughts on declustering in probabilistic seismic-hazard analysis, *Bull. Seismol. Soc. Am.* **104**, 1838–1845.

McGuire, R. K. (2004). Seismic Hazard and Risk Analysis, *Earthquake Engineering Research Institute*, MNO-10, Oakland, California.

Meletti, C., F. Galadini, G. Valensise, M. Stucchi, R. Basili, S. Barba, G. Vannucci, and E. Boschi (2008). A seismic source zone model for the seismic hazard assessment of the Italian territory, *Tectonophysics* **450**, 85–108.

Montaldo, V., E. Faccioli, G. Zonno, A. Akinci, and L. Malagnini (2005). Treatment of ground-motion predictive relationships for the reference seismic hazard map of Italy, *J. Seismol.* **9**, 295–316.

Reiter, L (1990). *Earthquake hazard analysis: issues and insig*hts. Columbia University Press, NY.

Stucchi, M., C. Meletti, V. Montaldo, H. Crowley, G. M. Calvi, and E. Boschi (2011). Seismic hazard assessment (2003–2009) for the Italian building code, *Bull. Seismol. Soc. Am.* **101**, 1885–1911.

Utsu, T. (1970). Aftershocks and earthquake statistics (1): Some parameters which characterize an aftershock sequence and their interrelations. *Journal of the Faculty of Science*, Hokkaido University, *Series 7, Geophysics* **3**, 129-195.

374 Utsu, T. (1961). A statistical study on the occurrence of aftershocks, *Geophys. Mag.* **30**, 521–605.
375 Yeo, G. L., and C. A. Cornell (2009). A probabilistic framework for quantification of aftershock ground-
376 motion hazard in California: Methodology and parametric study, *Earthq. Eng. Struct. D.* **38**, 455–
377 60.

Appendix

This appendix provides the derivation of aftershock disaggregation given in Equation (4). The symbols used in the derivation, some of which have been given already in the body of text, are as follows:

- v_E : mainshock (and sequence) occurrence rate;
- $M_E \in \left(m_{E,\min}, m_{E,\max}\right)$: mainshock magnitude;
- $M_A \in \left(m_{\min}, x\right)$: aftershock magnitude;
- $R_E \in \left(r_{E,\min}, r_{E,\max}\right)$: mainshock source-to-site distance;
- $R_A \in \left(r_{A,\min}, r_{A,\max}\right)$: aftershock source-to-site distance;
- $E\left[N_{A|x}\left(0,\Delta T_A\right)\right]$: mean number of aftershocks in a sequence of duration ΔT_A triggered by a mainshock of $M_E = x$;
- $E\left[N_{A,im|x}\left(0,\Delta T_A\right)\right]$: mean number of aftershocks exceeding the *im* threshold in a sequence of duration ΔT_A triggered maishock of $M_E = x$;
- λ_{im} : rate of exceedance of *im* according to SPSHA.
- IM_E : mainshock *IM*;
- IM_A : single aftershock *IM*;
- $IM_{\cup A}$: maximum aftershock *IM* in during a sequence.

It is sought the probability that, once exceedance of *IM* is observed, it is caused by an aftershock. Such a probability is formulated considering the following two events: (1) exceedance is observed and it could be possibly observed in the mainshock and/or during the aftershock sequence $\left(IM_E > im \cup IM_{\cup A} > im\right)$; (2) exceedance is observed in the aftershock sequence and it is not observed in the mainshock $\left(IM_E \le im \cap IM_{\cup A} > im\right)$. Consequently, the sough probability is: $P\left[IM_E \le im \cap IM_{\cup A} > im \middle| IM_E > im \cup IM_{\cup A} > im\right]$ that can be written as:

$$P\left[IM_E \le im \cap IM_{\cup A} > im \middle| IM_E > im \cup IM_{\cup A} > im\right] =$$

$$\frac{P\left[IM_E > im \cup IM_{\cup A} > im \middle| IM_E \le im \cap IM_{\cup A} > im\right] \cdot P\left[IM_E \le im \cap IM_{\cup A} > im\right]}{P\left[IM_E > im \cup IM_{\cup A} > im\right]} = , \quad \text{(A1)}$$

$$\frac{P\left[IM_E \le im \cap IM_{\cup A} > im\right]}{P\left[IM_E > im \cup IM_{\cup A} > im\right]}$$

where it is easy to recognize that $P\left[IM_E > im \cup IM_{\cup A} > im \middle| IM_E \le im \cap IM_{\cup A} > im\right] = 1$ given that exceedance has been observed during the aftershock sequence, it is certain that exceedance has been observed; i.e., the latter event is included in the former $\left(IM_E > im \cup IM_{\cup A} > im\right) \subseteq \left(IM_E \le im \cap M_{\cup A} > im\right)$. Now, applying the total probability theorem to the numerator of Equation (A1) gives,

$$\frac{P\left[IM_E \le im \cap IM_{\cup A} > im\right]}{P\left[IM_E > im \cup IM_{\cup A} > im\right]} = \frac{\iint_{M_E,R_E} P\left[IM_E \le im \cap IM_{\cup A} > im \mid x,y\right] \cdot f_{M_E,R_E}(x,y) \cdot dx \cdot dy}{P\left[IM_E > im \cup IM_{\cup A} > im\right]} =$$

$$\frac{\iint_{M_E,R_E} P\left[IM_E \le im \mid x,y\right] \cdot P\left[IM_{\cup A} > im \mid x,y\right] \cdot f_{M_E,R_E}(x,y) \cdot dx \cdot dy}{P\left[IM_E > im \cup IM_{\cup A} > im\right]} . \quad \text{(A2)}$$

In this latter equation, it is considered that the *IM*s of mainshocks and aftershocks are conditionally independent given the mainshock features (Yeo and Cornell, 2009).

It can be now recognized that the probability that exceedance of *IM* is not observed during the aftershock sequence is given by Equation (A3), which follows the NHPP assumption of APSHA (see Iervolino et al., 2014).

$$P\left[IM_{\cup A} > im \mid x,y\right] = 1 - e^{-E\left[N_{A,im|x}(0,\Delta T_A)\right]} = 1 - e^{-E\left[N_{A|x}(0,\Delta T_A)\right] \cdot \iint_{M_A,R_A} P\left[IM_A > im \mid w,z\right] \cdot f_{M_A,R_A|M_E,R_E}(w,z) \cdot dw \cdot dz} \quad \text{(A3)}$$

At this point, replacing Equation (A3) in Equation (A2), and multiplying numerator and denominator by ν_E, provides the sought result:

$$P\left[IM_E \le im \cap IM_{\cup A} > im \middle| IM_E > im \cup IM_{\cup A} > im\right] =$$

$$\frac{\nu_E}{\lambda_{im}} \cdot \iint_{M_E,R_E} P\left[IM_E \le im \mid x,y\right] \cdot \left(1 - e^{-E\left[N_{A|x}(0,\Delta T_A)\right] \cdot \iint_{M_A,R_A} P\left[IM_A > im \mid w,z\right] \cdot f_{M_A,R_A|M_E,R_E}(w,z) \cdot dw \cdot dz}\right) \cdot f_{M_E,R_E}(x,y) \cdot dx \cdot dy . \quad \text{(A4)}$$

The equation takes advantage of $\nu_E \cdot P\left[IM_E > im \cup IM_{\cup A} > im\right] = \lambda_{im}$. As a matter of fact, the rate of exceedance of im in SPSHA is the rate of occurrence of seismic sequences times the probability that a sequence causes at least one exceedance of im.

418 Table 1. Annual rates of mainshocks for the seismic source model of Figure 1.

	Magnitude												
	3.55-3.85	3.85-4.15	4.15-4.45	4.45-4.75	4.75-5.05	5.05-5.35	5.35-5.65	5.65-5.95	5.95-6.25	6.25-6.55	6.55-6.85	6.85-7.15	7.15-7.45
901	0	0	0.0153	0.0076	0.0166	0.0033	0.0021	0.0021	0	0	0	0	0
902	0	0	0.0534	0.0153	0.0166	0.0099	0	0.0064	0.0014	0	0	0	0
903	0	0	0.0992	0.0076	0.0099	0	0	0.0021	0	0	0	0	0
904	0	0	0.0305	0.0153	0	0	0.0042	0	0	0	0	0	0
905	0	0	0.1687	0.0904	0.0254	0.0106	0.0085	0.0071	0	0.0033	0.0022	0	0
906	0	0	0.0663	0.0482	0.0127	0.0021	0.0042	0	0	0.0011	0	0	0
907	0	0	0.0302	0.0301	0.0021	0	0.0021	0.0014	0	0	0	0	0
908	0	0	0.1069	0.0076	0.0166	0.0066	0.0021	0	0	0	0	0	0
909	0	0	0.0305	0.0076	0.0099	0.0066	0.0021	0	0	0	0	0	0
910	0	0	0.0611	0.0076	0	0.0066	0.0021	0.0064	0	0.0014	0	0	0
911	0	0	0.0305	0.0076	0.0099	0	0.0021	0	0	0	0	0	0
912	0	0	0.0482	0.0120	0.0106	0.0148	0.0021	0.0028	0.0012	0	0	0	0
913	0	0	0.1145	0.0602	0.0169	0.0042	0.0085	0.0014	0	0	0	0	0
914	0	0	0.0843	0.0663	0.0148	0.0085	0.0021	0.0057	0.0014	0	0	0	0
915	0	0	0.1832	0.0763	0.0398	0	0.0042	0.0042	0.0014	0.0014	0	0	0
916	0	0	0.0458	0.0305	0.0085	0.0042	0.0021	0	0	0	0	0	0
917	0	0	0.0542	0.0301	0.0114	0.0085	0.0106	0.0064	0.0012	0	0	0	0
918	0	0	0.1527	0.0229	0.0170	0.0057	0.0085	0.0064	0.0042	0.0014	0	0	0
919	0	0	0.1298	0.0534	0.0297	0.0106	0.0042	0.0071	0.0043	0.0025	0	0	0
920	0	0	0.1832	0.0687	0.0568	0.0085	0	0	0	0	0	0	0
921	0	0	0.1756	0.0840	0.0254	0.0085	0.0021	0.0028	0	0	0	0	0
922	0	0	0.0458	0.0229	0.0169	0.0042	0	0	0	0	0	0	0
923	0	0	0.4122	0.0992	0.0767	0.0227	0.0085	0.0106	0.0021	0.0057	0.0043	0.0014	0.0014
924	0	0	0.0687	0.0382	0.0372	0.0279	0.0140	0	0.0042	0	0.0017	0	0
925	0	0	0.0458	0.0153	0.0047	0	0	0	0	0.0033	0.0017	0	0
926	0	0	0.0305	0.0076	0.0186	0	0.0047	0	0	0	0	0	0
927	0	0	0.2150	0.0561	0.0512	0.0093	0.0047	0.0064	0.0021	0.0042	0.0066	0.0066	0
928	0	0	0.0154	0.0153	0.0186	0	0.0042	0.0021	0	0	0	0	0
929	0	0	0.2243	0.0374	0.0651	0.0186	0.0140	0.0140	0.0085	0.0021	0.0017	0.0066	0.0017
930	0	0	0.1028	0.0093	0.0047	0.0093	0.0093	0.0047	0.0021	0.0021	0.0017	0	0
931	0	0	0.0193	0.0192	0	0	0.0047	0	0	0	0	0.0021	0
932	0	0	0.0748	0.0187	0.0166	0.0033	0	0	0.0042	0	0	0	0
933	0	0	0.1145	0.0153	0.0132	0.0199	0.0066	0.0021	0.0021	0	0	0	0
934	0	0	0.0280	0.0001	0.0099	0.0033	0	0	0.0021	0	0	0	0
935	0	0	0.0534	0.0001	0.0166	0.0099	0.0042	0	0.0021	0	0.0023	0	0.0012
936	0.3359	0.0458	0.0382	0.0153	0.0132	0.0033	0	0	0	0	0	0	0

419

420 Table 2. Nationwide percentage and maximum increase of *im* of SPSHA with respect to PSHA.

	PGA				*Sa*(1s)			
T_r [yr]	50	475	975	2475	50	475	975	2475
Ave. perc. diff. [%]	9.7	10.1	10.3	9.8	10.4	8.7	8.0	7.0
Max. perc. diff. [%]	16.4	22.3	25.6	27.9	16.2	16.7	16.6	14.8
Max. abs. diff. [g]	0.012	0.058	0.084	0.116	0.007	0.035	0.051	0.075

421

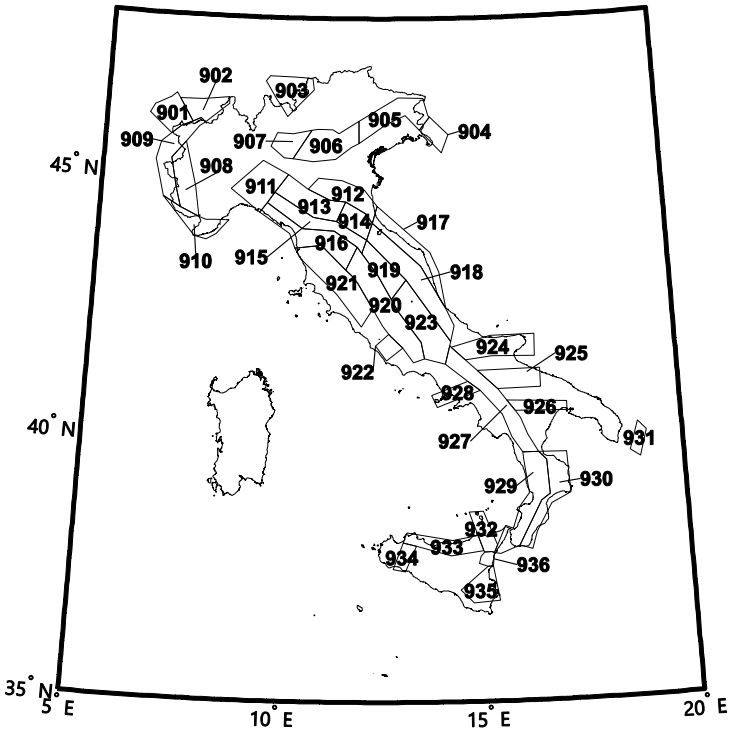

Figure 1. The seismic source zone model for Italy, according to the model of Meletti et al. (2008).

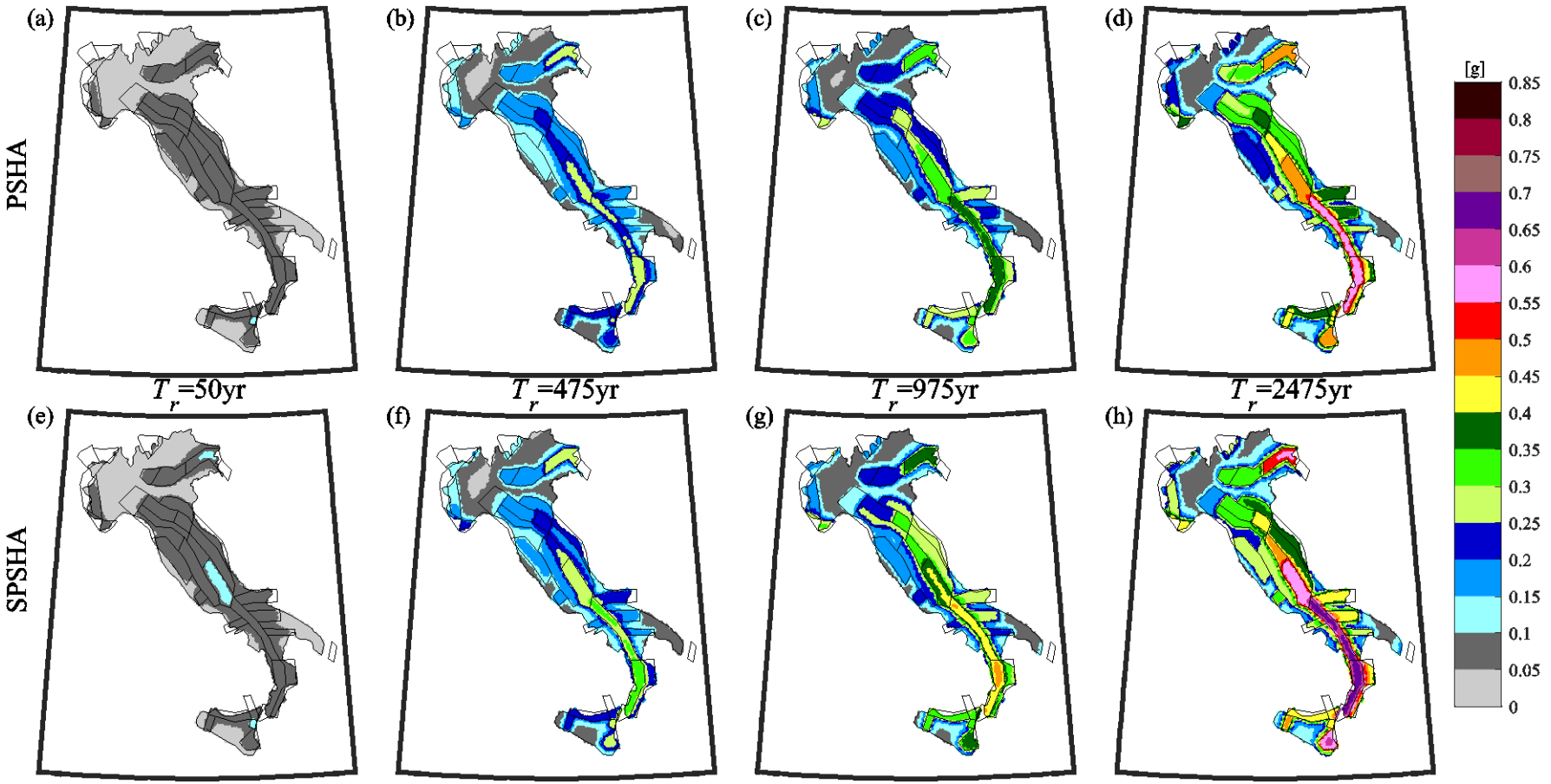

Figure 2. Maps of PGA: *im* on rock with four return periods of exceedance equal to: 50yr, 475yr, 975yr and 2475yr. Panels from (a) to (d) are computed via PSHA, (e) to (h) are computed via SPSHA.

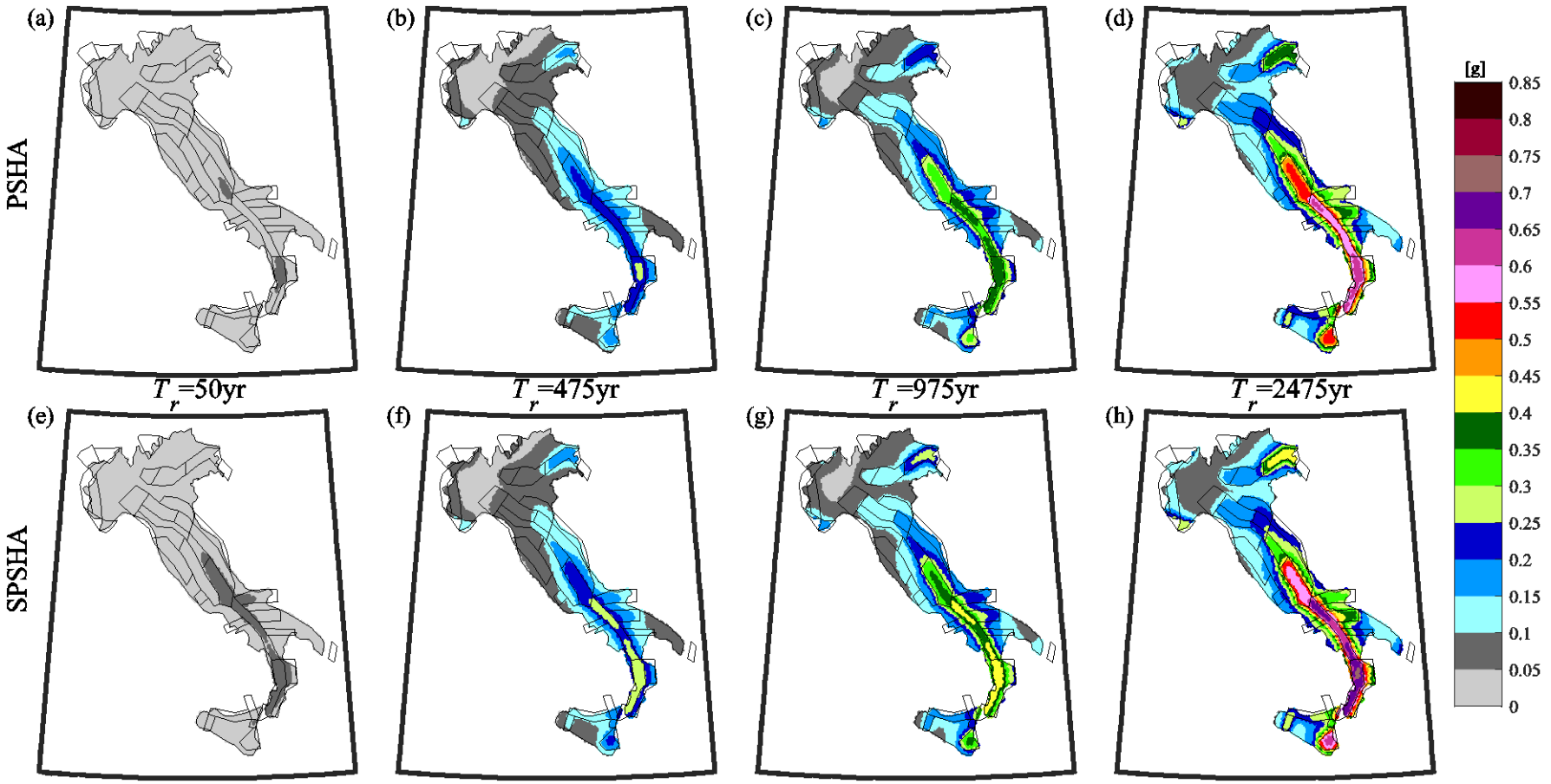

Figure 3. Maps of $Sa(1s)$: *im* on rock with four return periods of exceedance equal to: 50yr, 475yr, 975yr and 2475yr. Panels from (a) to (d) are computed via PSHA, (e) to (h) are computed via SPSHA.

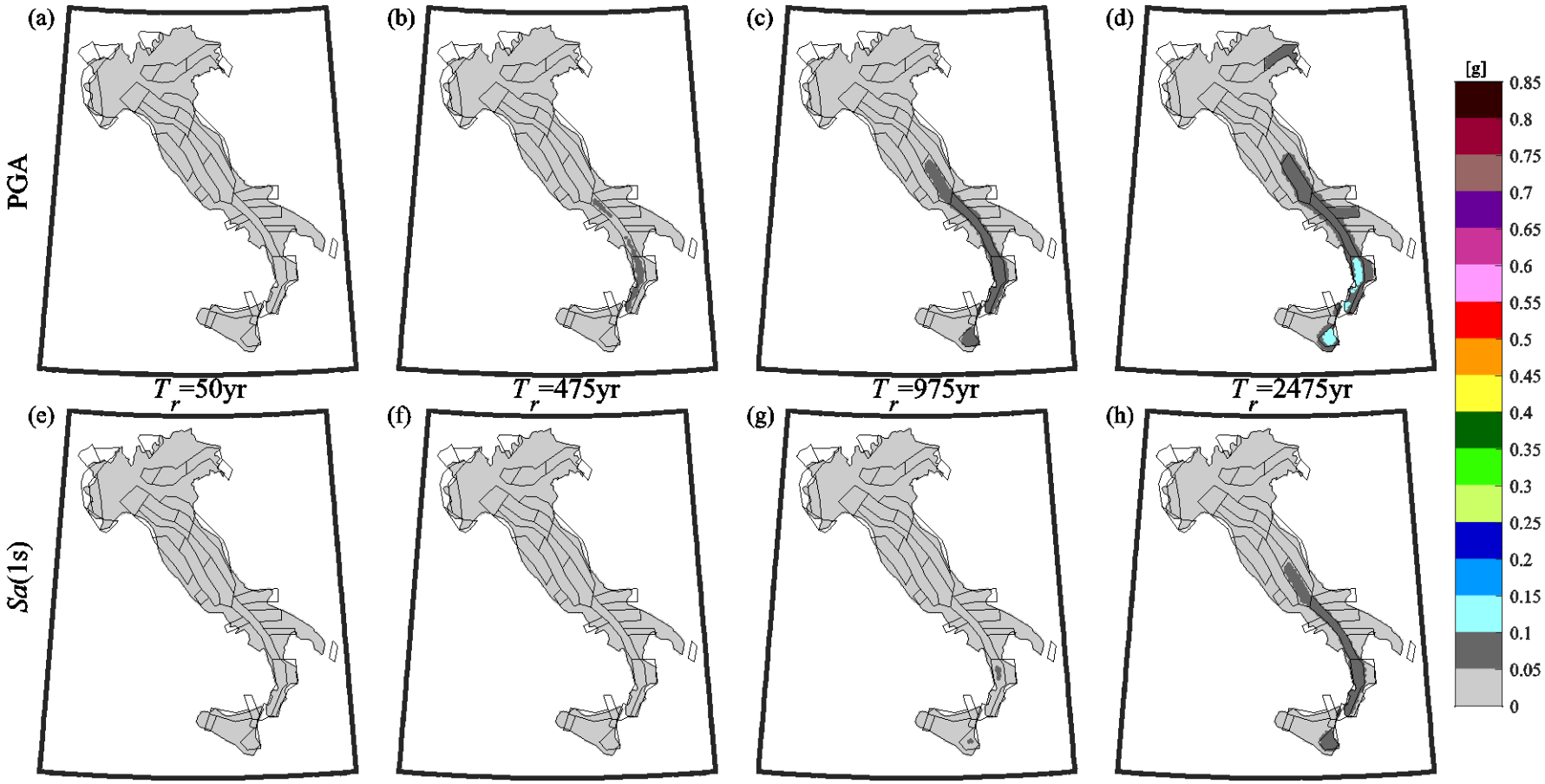

Figure 4. Differences between SPSHA and PSHA in terms of *im* with 50yr, 475yr, 975yr and 2475yr return periods of exceedance on rock. Panels from (a) to (d) are PGA, from (e) to (h) are $Sa(1\text{s})$.

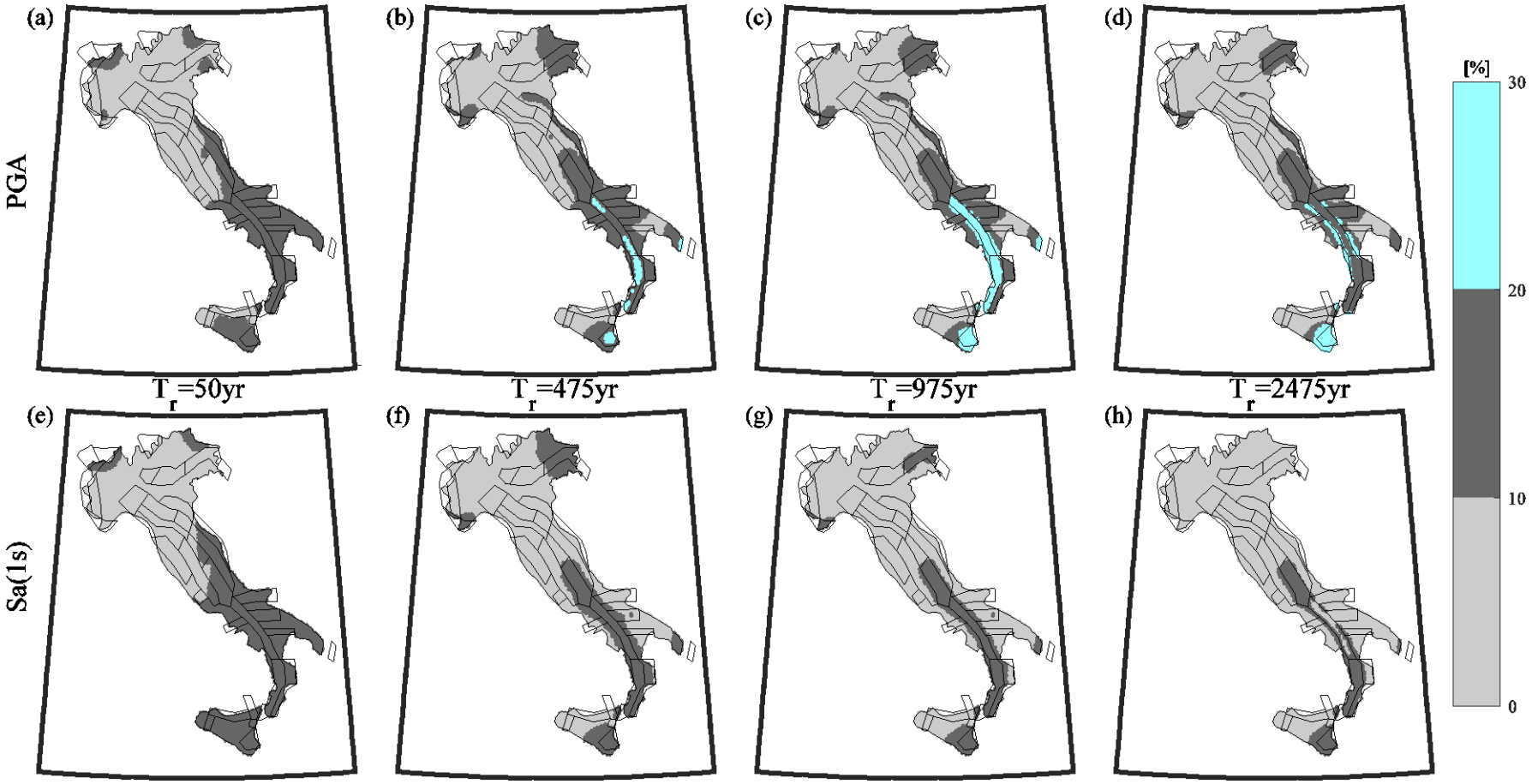

Figure 5. Percentage increase from SPSHA with respect to PSHA in terms of im with 50yr, 475yr, 975yr and 2475yr return periods of exceedance on rock. Panels from (a) to (d) are PGA, from (e) to (h) are $Sa(1s)$.

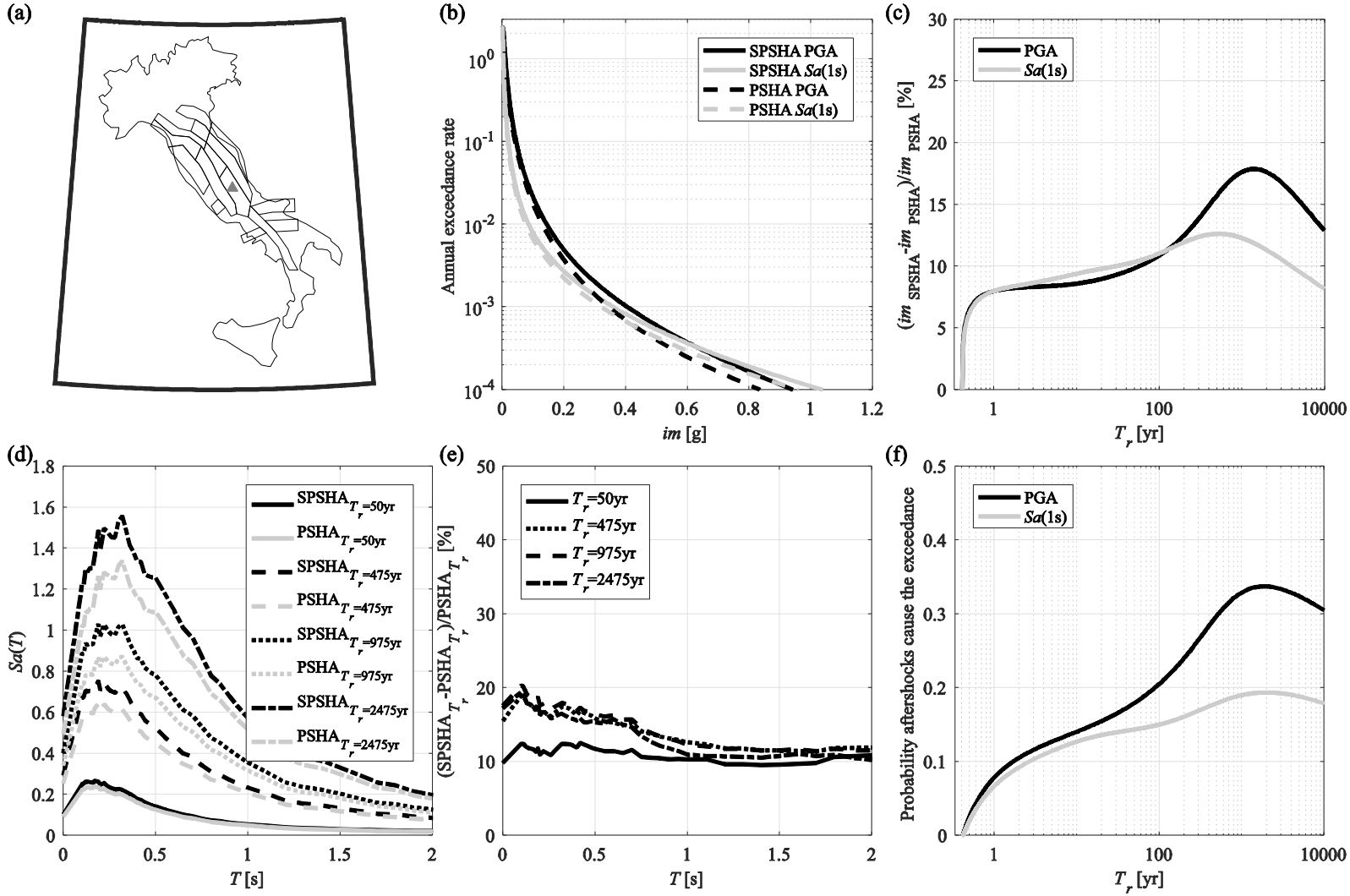

Figure 6. Results of hazard analyses for L'Aquila: (a) location of the site and source zones contributing to its hazard; (b) hazard curves for PGA and $Sa(1\text{s})$; (c) hazard increase as a function of the exceedance rate of im; (d) UHS for 50yr, 475yr, 975yr and 2475yr; (e) hazard increase as a function of the spectral period and for fixed return periods; (f) aftershock disaggregation for PGA and $Sa(1\text{s})$.

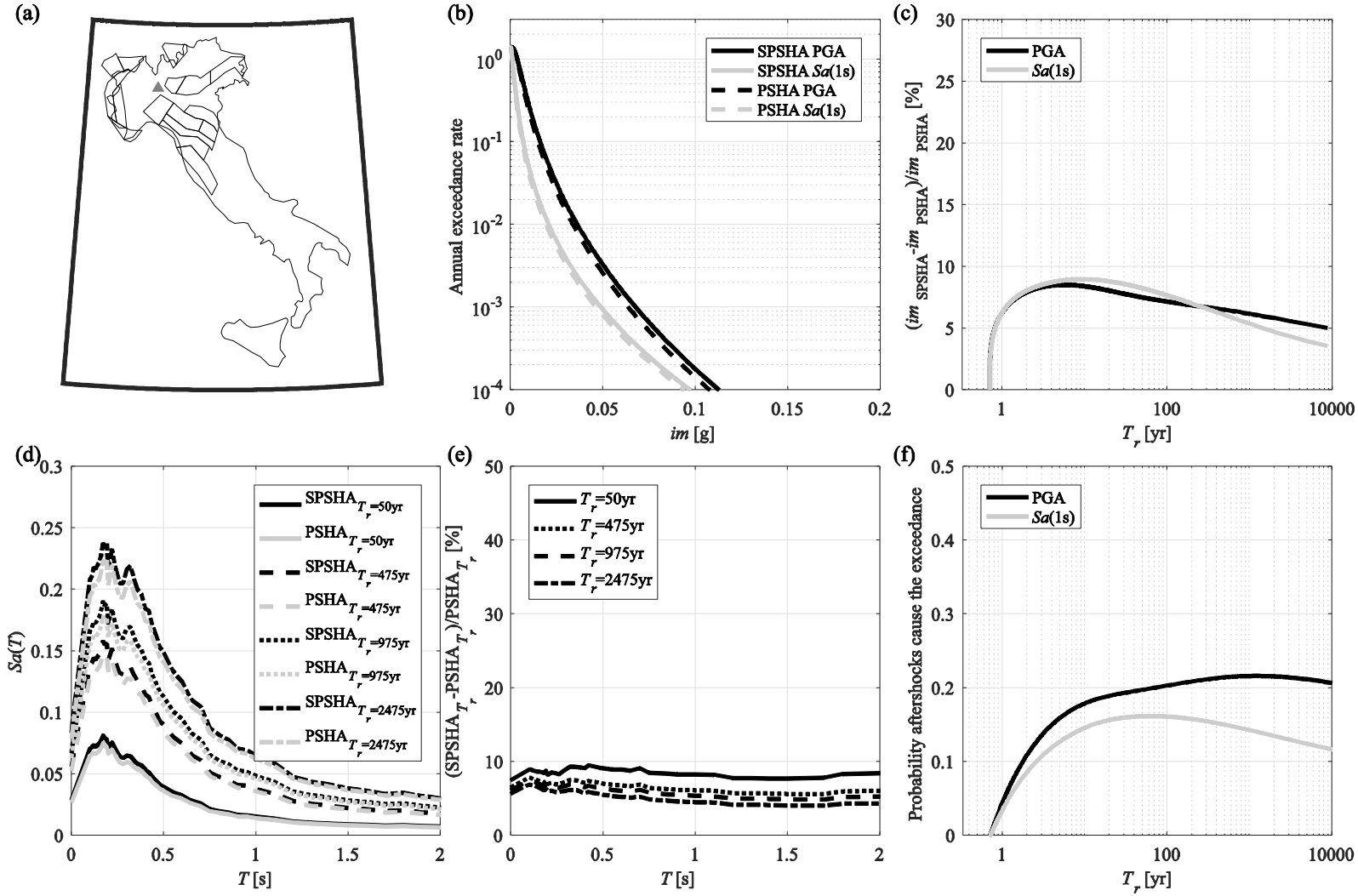

Figure 7. Results of hazard analyses for Milan: (a) location of the site and source zones contributing to its hazard; (b) hazard curves for PGA and $Sa(1\text{s})$; (c) hazard increase as a function of the exceeding rate of the im; (d) UHS for 50yr, 475yr, 975yr and 2475yr years; (e) hazard increase as a function of the spectral period and for fixed return periods; (f) aftershock disaggregation for PGA and $Sa(1\text{s})$.